

# Hydrogel Lasers Via Supramolecular Host–Guest Complexation

Matias Paatelainen, Markus Lahikainen, Alex Berdin, Kim Kuntze, Werner M. Nau, Nonappa, and Arri Priimagi\*

Supramolecular host–guest complexes are dynamic systems composed of typically macrocyclic host molecules encapsulating smaller guest molecules. One of their applications is the selective encapsulation of fluorescent dye molecules to tackle quenching and photobleaching in solution. When extended to solid matrices, the efficiency of dyes can be especially poor, limiting their use in fluorescence-based applications. Here it is demonstrated that supramolecular host–guest complexation in a hydrogel network allows readily tunable hydrogel-based lasers. Poly(*N*-isopropylacrylamide)-based copolymer hydrogel is used with covalently linked Rhodamine B molecules. By controlled doping of cucurbit[7]uril as a host molecule in the hydrogel, it is shown that the fluorescent quantum yield increases from 17% to 51%, accompanied by 15-fold enhancement in photostability. As proof of concept, a thin-film distributed feedback hydrogel laser with wavelength tunability is fabricated. The results reveal a 30% increase in slope efficiency in the presence of host molecules. These results, combined with the inherent stimuli-response of hydrogels, enable new possibilities for affordable and small-scale photonic devices capable of safely interacting with the environment in, for example, sensing applications.

release, responsive adhesives, and artificial muscles.<sup>[1–5]</sup> They comprise a guest molecule, which is encapsulated by a larger, typically ring- or cylinder-shaped host molecule. Intermolecular interactions responsible for holding these systems together can be, for example, hydrogen bonding, van der Waals forces, hydrophobic/solvophobic effects, or a combination of these.<sup>[6]</sup> Being dynamic in nature, host–guest complexes allow the design of stimuli-responsive functional systems that can be controlled with, for example, light, temperature, and pH.<sup>[7–9]</sup>

One specific application of supramolecular host–guest complexes is the control over the photophysical properties of light-emitting dyes.<sup>[10]</sup> Organic dyes with distinct photoluminescent properties are used as stains and probes in bioimaging,<sup>[11]</sup> molecular recognition and tagging,<sup>[12]</sup> and as emission sources in organic lasers.<sup>[13]</sup> The versatility and abundance of dyes, broad emission and absorption spectra, and modifiability make them affordable, flexible, and

integrable light sources. However, dyes in general suffer from aggregation and photobleaching, typically contributing negatively to fluorescence emission.<sup>[13]</sup> Aggregation is prominent at high concentrations and in polar solvents, such as water, and often leads to fluorescence quenching.<sup>[14]</sup> Photobleaching refers to the depletion of fluorescent species under optical pumping through inter- or intramolecular reactions that modify the chromophore structure.<sup>[15]</sup> Host–guest complexation between dyes and macrocycles can be used to hinder both of these undesirable phenomena. Encapsulation of the dye molecules prevents aggregation by providing an isolated and confined microenvironment, simultaneously promoting radiative relaxation, and hindering photobleaching.<sup>[16]</sup> Modification of fluorescence through supramolecular host–guest complexation can thus enhance emission,<sup>[10]</sup> provide designs for fluorescent probes,<sup>[16]</sup> and improve dye laser performance.<sup>[17,18]</sup>


Dye laser development is an active research area, which is driven by their superior properties as light sources compared to those exhibiting spontaneous emission, such as high intensity, directionality, coherence, and superior spectral resolution.<sup>[13,19,20,21]</sup> Dye lasers also offer broad wavelength tunability, making them attractive for, e.g., spectroscopy and analytical devices.<sup>[22]</sup> Host–guest complexation has enabled efficient

## 1. Introduction

Supramolecular host–guest complexes offer considerable potential in utilizing precisely assembled structures in a variety of different applications, such as chemosensors, controlled drug

M. Paatelainen, M. Lahikainen, A. Berdin, K. Kuntze, Nonappa, A. Priimagi  
Faculty of Engineering and Natural Sciences  
Tampere University  
Tampere 33230, Finland  
E-mail: arri.priimagi@tuni.fi

W. M. Nau  
School of Science  
Constructor University  
28759 Bremen, Germany

 The ORCID identification number(s) for the author(s) of this article can be found under <https://doi.org/10.1002/adom.202300232>

© 2023 The Authors. Advanced Optical Materials published by Wiley-VCH GmbH. This is an open access article under the terms of the Creative Commons Attribution License, which permits use, distribution and reproduction in any medium, provided the original work is properly cited.

DOI: 10.1002/adom.202300232

dye lasers in aqueous solutions with improved beam characteristics compared to organic solvent-based systems.<sup>[17,18,23]</sup> However, liquid dye lasers are limited by their structural complexity and health/safety/sustainability issues related to the use of dye solutions. Polymer-based solid-state dye lasers provide a way to bypass these limitations along with intriguing advantages. The use of polymeric host matrices for dyes allows straightforward and low-cost manufacturing of miniaturized flexible devices that can be diversely used for integrated photonics in, for example, lab-on-a-chip and microfluidic systems.<sup>[20]</sup> The wavelength tunability/sensitivity can be achieved by designing integrated and controllable resonator structures, for example, distributed feedback (DFB) configurations, where emission wavelength is selected by periodic modulation of gain or refractive index.<sup>[24]</sup> Polymer matrices provide support for laser structures while allowing reversible control over the DFB structure (and hence wavelength tuning of the laser emission) via, for example, mechanical deformation or, in case of cholesteric liquid crystal (CLC) lasers, tuning the pitch of the polymerized CLC.<sup>[25,26,27,28]</sup> The periodic structure can be generally produced inexpensively and without complex processes, for example through surface relief gratings (SRG) via photo- and soft-lithographic methods.<sup>[29,30]</sup> However, photobleaching and aggregation are critical problems particularly in solid-state dye lasers as highly concentrated and non-replenishable gain media without adequate cooling are exposed to intense pump irradiation.<sup>[31]</sup> Supramolecular host-guest complexes could offer an effective solution to these problems while preserving the advantages related to organic materials.

When aiming for combining the advantages of solid-state dye lasers and host-guest complexation, hydrogels may prove to be a desirable platform. As 3D networks capable of absorbing high amounts of water, hydrogels can provide heat dissipation and structural simplicity. Considering the tunability and controllability, swelling/deswelling induces changes in dimensions and possible topographical patterns altering the light propagation,<sup>[32]</sup> which can be triggered by external stimuli such as temperature,<sup>[33]</sup> light,<sup>[34]</sup> pH,<sup>[35]</sup> or analytes.<sup>[36]</sup> Furthermore, the resemblance of hydrogels to biological tissue allows them to encapsulate and provide a natural environment for cells and biomolecules. The water content of the hydrogel network and possible encapsulated compounds affect the lasing properties, for example, threshold, modes, and spectra, making hydrogels a tempting platform for sensing or controlling lasing based on biological reactions and systems, as has been shown previously in the context of hydrogel microcavity lasers.<sup>[37,38]</sup> By constructing integrated laser resonators from hydrogels, remotely tunable and responsive lasers exclusive of complicated frameworks could be realized. Furthermore, if the dye and host are attached to the hydrogel matrix, the laser in its completeness can be directly exposed to and affected by the surrounding medium, for example, analyte solution in the case of optofluidic devices, without concern of contamination. This would allow the use of such devices as integrated sensors<sup>[39]</sup> or probes<sup>[40]</sup> in biomedical applications. By using non-cytotoxic and biodegradable material constituents, possibilities could be extended even to wearable and implantable photonic devices. Finally, the high heat capacity of aqueous media and associated low thermal refractive index dependence should have beneficial effects on potential lasing properties, prominently

the beam shape, as heat related to incident radiation is effectively dissipated.

In this article, we exploit the concept of supramolecular host-guest complexation in a hydrogel network using cucurbit[7]uril (CB7) as a host molecule and acrylated Rhodamine B (RhBa) as a fluorescent dye in a poly(*N*-isopropylacrylamide) (PNIPAm) hydrogel. RhBa was attached covalently to the polymer matrix and the host was added through diffusion by swelling the hydrogel. Complexation between CB7 and RhBa led to an enhancement of fluorescence as well as improved photostability in swollen hydrogel films. As a demonstration of possible devices, we fabricated a wavelength-tunable thin-film DFB laser from the studied hydrogel via photo- and soft lithographic methods.

## 2. Results and Discussion

### 2.1. Materials Design

The material design is based on a cross-linked PNIPAm-co-acrylic acid hydrogel with covalently attached RhBa fluorescent dye and doped CB7 macrocyclic host molecule (see the Experimental Section for further details). PNIPAm is a widely used thermoresponsive hydrogel where hydrophilic amide groups of the monomer absorb water and result in macroscopic volume changes.<sup>[41]</sup> Swelling displays temperature dependence with threshold behavior at lower critical solution temperature (LCST)  $\approx 32$  °C.<sup>[42]</sup> Below LCST PNIPAm is miscible in water, but above has a turbid appearance. LCST can be manipulated by hydrophobic and/or hydrophilic additives, and the swelling can be controlled by the number of cross-links. A higher number of cross-links leads to decreased swelling and slower diffusion owing to hindered movement of the polymer chains and increased density.<sup>[43,44]</sup> As it simultaneously restricts the swelling and therefore the refractive index decrease based on water uptake, which is essential for the film laser waveguide structure, both factors were considered for choosing the optimal cross-linker concentration.<sup>[45]</sup> On the other hand, acrylic acid increases the hydrophilicity of the polymer network, raising the LCST and increasing the swelling ability.<sup>[46]</sup> The hydrogel composition was adjusted so that swelling could be reached underwater in ambient conditions. The hydrogels were synthesized in a closed glass cell via photoinitiated free-radical polymerization. The introduction of the host molecule into the system was achieved through diffusion by immersing and swelling the hydrogel in an aqueous CB7 solution. **Figure 1** shows the material design and illustrates the complexation.

### 2.2. Photoluminescence Enhancement

To confirm the applicability of the modified rhodamine dye, the RhBa•CB7 complex formation was first studied in an aqueous solution (**Figure 2a**). Fluorescence emission intensity was measured from a 2  $\mu$ m aqueous solution of RhBa with CB7 concentrations ranging from 0 to 40  $\mu$ m. Upon CB7 addition, a significant increase in fluorescence intensity was initially observed with subsequent gradual saturation. This is a consequence of CB7-encapsulated monomeric RhBa species which is known to exert higher luminescence in aqueous media.<sup>[18]</sup> The water initially

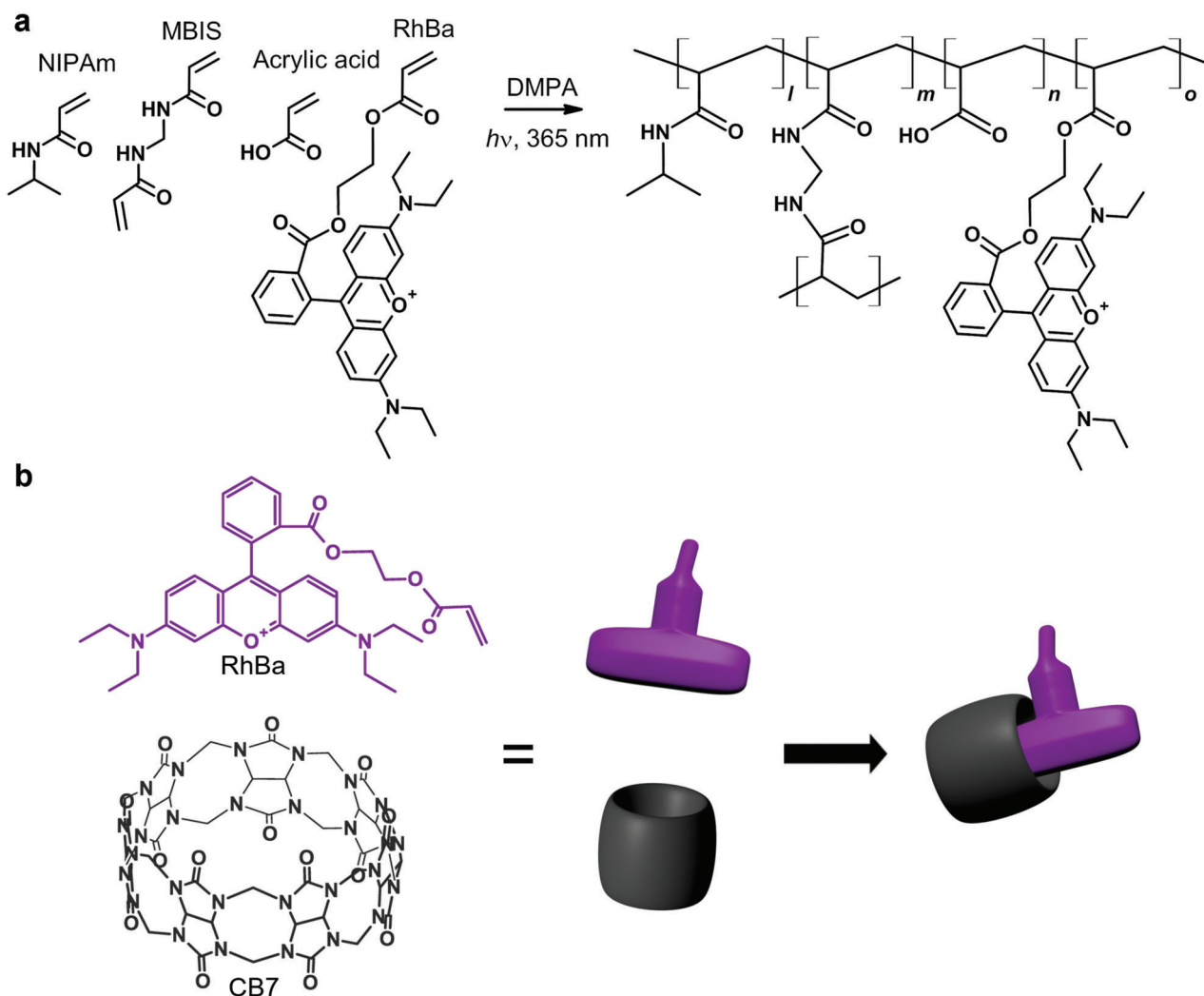


**Figure 1.** Hydrogel synthesis and complexation scheme. a) Chemical structures of the monomers used and the resulting random copolymer. b) Chemical structures of RhBa and CB7 with schematics of the host-guest complex.

occupying the hydrophobic cavity of CB7 is replaced by the energetically more favorable guest, in this case, one of the diethylamino aryl rings of RhBa.<sup>[47]</sup> The binding affinity between RhBa and CB7 in an aqueous solution was estimated by expressing the change in fluorescence intensity with CB7 concentration, as shown in the inset of Figure 2a (see Equations S1 and S2, Supporting Information for further details).<sup>[48]</sup> The data can be represented by a 1:1 complexation model and a relatively high association constant of  $K_{eq} = 8.8 \cdot 10^5\text{ M}^{-1}$  can be extracted, which is consistent with literature and indicates a rather stable supramolecular complex.<sup>[18]</sup>

The host-guest complexation in the hydrogel matrix was studied by absorption and emission spectroscopy. Figure 2b shows the normalized absorption spectra of dry and swollen hydrogel in the absence and presence of CB7. The absorption spectrum of dry hydrogel peaks at 560 nm and has a modest, blue-shifted shoulder at 530 nm. When immersed in water the shoulder peak becomes more prominent, which can be attributed to parallel-organized H-dimers of RhBa.<sup>[49]</sup> Upon addition of CB7,

the shoulder is suppressed and the original spectrum is retained, indicating that RhBa aggregates are dismantled as the host-guest complex formation takes place. Similar changes can be observed in a concentrated solution as shown in Figure S1 (Supporting Information), supporting the reasoning that the complexation occurs homogeneously in the hydrogel and not only on the surface. Subsequent removal of water in hydrogel leads to the emergence of a broader shoulder peak, which might be caused by a partial disintegration of the complexes and the re-formation of aggregates.

The effect of host-guest complexation on light emission from hydrogels was studied using fluorescence spectroscopy. The time to reach equilibrium was determined by monitoring saturation of the fluorescence emission from hydrogel immersed in CB7 solution (Figure S2, Supporting Information). The increase in the RhBa concentration increased the emission intensity change along with host addition because of initially higher number of aggregates (Figure S3, Supporting Information). RhBa concentration of 0.5 mol-% was chosen based on a clear increase in

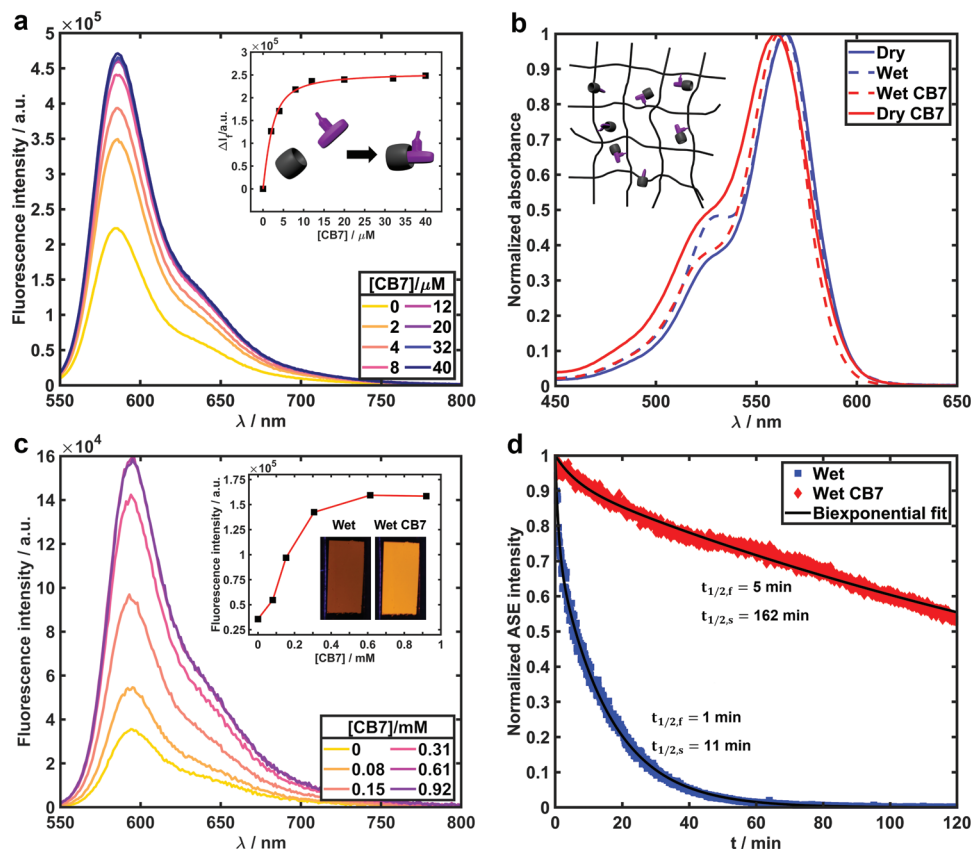


**Figure 2.** Fluorescence enhancement via host-guest complexation. a) Fluorescence emission intensity of 2  $\mu\text{M}$  RhBa solution with increasing concentration of CB7. Inset shows the peak emission intensity as a function of CB7 concentration; black squares correspond to experimental data and the red solid line to a theoretical fit for 1:1 complexation. b) Absorption spectra of a hydrogel film in wet and dry states in the presence and absence of CB7. c) Fluorescence emission spectra from a hydrogel film immersed in a CB7 solution with a concentration of 0–0.9 mM. Inset shows the change in peak emission intensity against CB7 concentration and photographs of a sample under UV illumination in water and in CB7 solution. d) Amplified spontaneous emission decay curves from a hydrogel in water and in CB7 solution with half-lives extracted from biexponential fit.

the fluorescence intensity upon complexation. Figure 2c shows the fluorescence emission spectra of 10  $\mu\text{m}$  thick hydrogel film swollen in 0.8 mL of CB7 solutions with concentrations ranging from 0–0.9 mM. The emission intensity increases with CB7 concentration and saturates to a value 5 times higher than the initial level in water, causing a visible change in emission under UV excitation (Figure 2c inset). Similarly, the fluorescence quantum yield increases from 17% to 51% upon host addition (Figure S4, Supporting Information). The increase in fluorescence intensity and quantum yield suggests that host-guest complexation is favored in swollen hydrogels and converts weakly fluorescent dye aggregates into strongly fluorescent monomeric species.

CB7 is known to enhance the photostability of encapsulated fluorescent dyes<sup>[50,51]</sup> that is essential for advanced applications such as their use as fluorescent markers<sup>[50,52]</sup> or as lasing material.<sup>[17,18]</sup> Accordingly, the photostability of the material was studied by monitoring the output intensity of amplified spontaneous emission (ASE), which is produced by stimulated emission and resembles closely the conditions exerted on the material under optical pumping required for lasing.<sup>[53]</sup> The decay curves in Figure 2d show that the photostability of the system improves significantly in the presence of CB7. The results are best described with a biexponential fit, which suggests

that two species decaying at different rates are contributing to emission, as described in the literature, for example, for fluorescein in poly(vinyl alcohol) matrix (See Equation S6 and Table S1, Supporting Information).<sup>[15]</sup> Herein the two species would possibly translate to monomeric/encapsulated (slow decay) and aggregated (fast decay) dye molecules. The contribution and half-life of the slow decay component increase from 74% to 93% and from 11 min to 162 min, respectively, upon supramolecular encapsulation. This demonstrates an impressive increase in photostability by a factor of at least 15, as judged by the effect on ASE (Figure 2d). The decreased contribution of the fast decay component suggests the deaggregation of dye molecules due to host-guest complexation as aggregates are more prone to photobleaching than monomeric species.<sup>[15]</sup> In addition, the encapsulation-induced isolation and protection against photodegradation mechanisms, for example, reactions with oxygen, water, or adjacent dye molecules, may contribute to the increased half-life.

### 2.3. Hydrogel Laser Design and Fabrication

A thin film DFB laser structure is a slab waveguide with periodic modulation of either gain, refractive index, or both, i.e., a diffract-



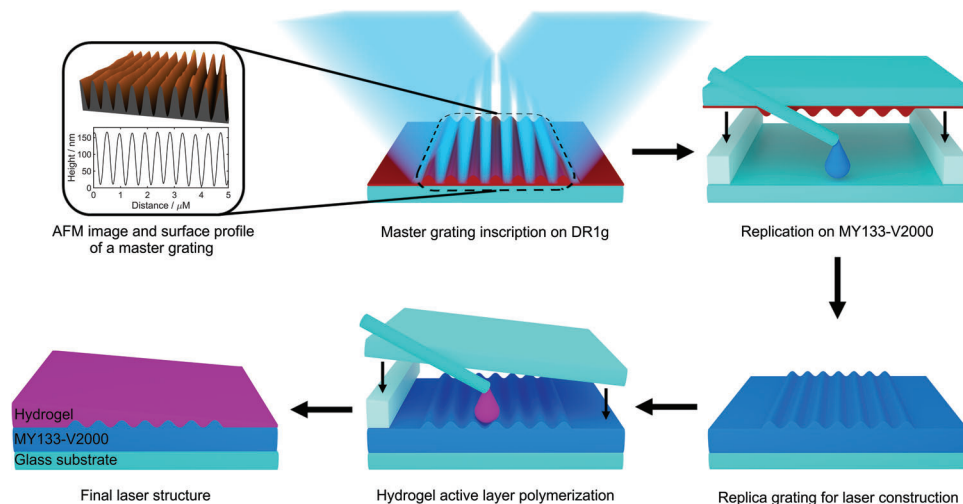


**Figure 3.** Hydrogel laser fabrication process. An SRG is inscribed on a DR1g film using holographic lithography, 3D AFM image (top) and surface profile (bottom) of the master SRG is shown on the left. The grating is replicated on MY133-V2000 via soft lithography in a glass cell with 50  $\mu\text{m}$  spacers. The replica grating is used to construct a polymerization cell for the hydrogel layer with a 1  $\mu\text{m}$  PDMS spacer on one side. As a result, a DFB laser structure with grating between the slanted hydrogel layer and MY133-V2000 layer is produced.

tion grating. According to the coupled wave theory by Kogelnik and Shank,<sup>[24]</sup> the waves are coupled by the grating which leads to distributed optical feedback. The emission wavelength  $\lambda$  of the DFB laser is governed by the Bragg equation

$$m\lambda = 2n_{\text{eff}}\Lambda \quad (1)$$

where  $m$  is the diffraction order,  $n_{\text{eff}}$  is the effective refractive index of the waveguide and  $\Lambda$  is the grating period. The outcoupling of the laser depends on the diffraction order, the frequently used ones being  $m = 1$  and  $m = 2$  which result in emission from the edge and to the direction of the surface normal, respectively. Surface emission offers simple outcoupling of light for analysis and therefore the second-order design was chosen in this work. The periodic structure was introduced in the form of SRGs inscribed on an azobenzene-containing photoactive material, as has been previously used in the context of DFB lasers.<sup>[25,54,55]</sup> The laser fabrication process is illustrated in **Figure 3**. In the first step, Disperse Red 1-glass (DR1g) thin film on a glass substrate was exposed to an interference pattern on Lloyd's mirror setup.<sup>[56]</sup> Azobenzene moieties undergo alternating *cis-trans* isomerization cycles in the high-intensity regions, which causes them to migrate to low-intensity areas and create periodic surface corrugation.<sup>[57]</sup> The second step involved the replication of the master grating on a low refractive index polymer MY133-V2000 ( $n = 1.33$ ), which transferred the grating to the laser and acted as a bottom cladding. Finally, the hydrogel layer was polymerized on top of the replica in a closed cell with a 1  $\mu\text{m}$  thick PDMS spacer stripe on one side. As a result, the active hydrogel layer had a slanted geometry that allows wavelength selection based on the thickness gradient along the film. In its completeness, the laser consisted of the bottom cladding and the active hydrogel layer with the grating in between, and eventually water as the top cladding. The refractive index of swollen PNIPAM is 1.52–1.33 depending on the water content of the hydrogel.<sup>[45]</sup> For current

material in the swollen state, the refractive index was estimated to be 1.39 at 589.3 nm using a refractometer.

#### 2.4. Hydrogel Laser Characterization

The optical amplification of the material was determined using the variable stripe length (VSL) method, where a sample is pumped with a stripe-shaped beam (**Figure 4a** inset).<sup>[58]</sup> The optical gain region sets between 610–670 nm according to normalized amplification measured from a featureless waveguide, as shown in **Figure 4a**. The gain at the peak amplification increased by 20% along CB7 addition, due to the deaggregation of RhBa and thus reduced quenching (**Figure S5**, Supporting Information). However, the absolute gain values should be interpreted with care due to uncertainties and limitations related to the VSL method.<sup>[58]</sup>

Based on the gain curves and refractive index profile of the waveguide, a hydrogel laser with a grating period of 468 nm was fabricated (**Figure S6**, Supporting Information) to set the laser emission wavelength to coincide with the highest amplification. The measurements were conducted for the swollen hydrogel in water. **Figure 4b** shows the difference between fluorescence, ASE, and laser emission. First, the ASE leads to a spectral narrowing at the right shoulder of the fluorescence spectrum. Finally, a sharp laser emission peak appears at 630 nm due to the feedback provided by the grating. The full width at half maximum of the laser peak was measured at 0.2 nm, which is at the resolution limit of the spectrometer used. The inset shows a narrow line-shaped emission characteristic of second-order DFB laser.<sup>[19]</sup> In a surface-emitting DFB laser with 1D grating the mode confinement is restricted in the direction parallel to the grating vector, allowing higher beam divergence along the grating lines.

**Figure 4c** shows the lasing efficiency with and without the host, measured by the output energy as a function of the input energy. For a reliable comparison between the two systems, the

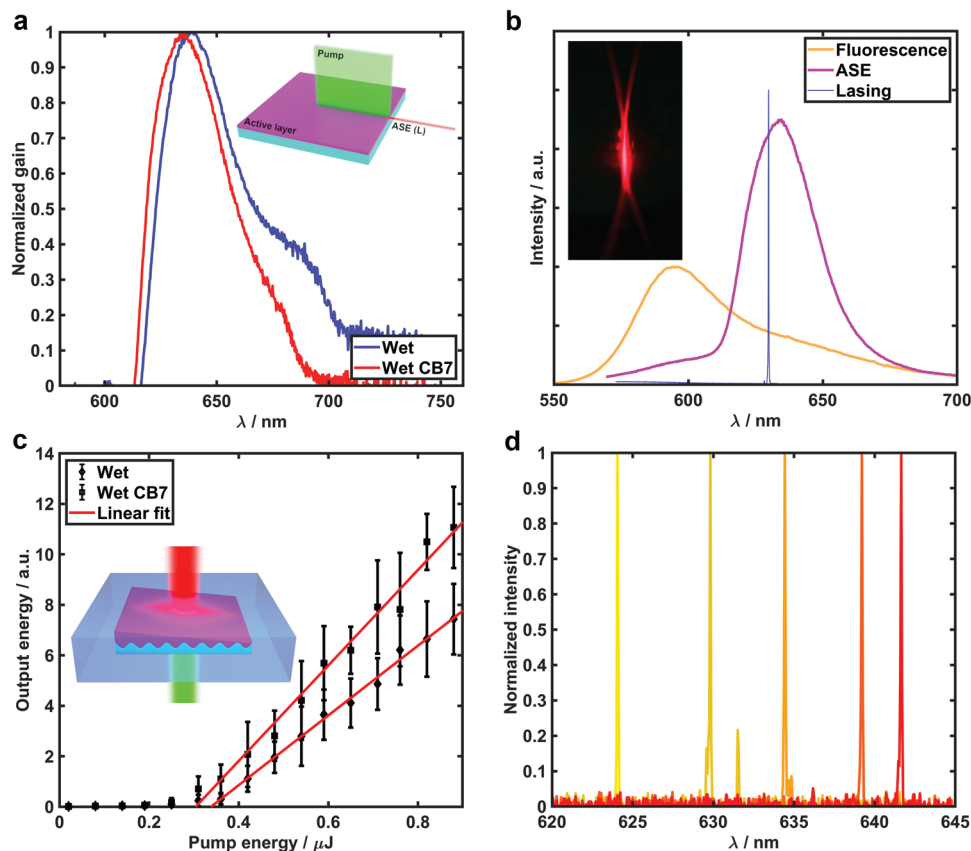


**Figure 4.** Toward thin film hydrogel laser. a) Normalized gain curves of hydrogel film on MY133-V2000 substrate in water and CB7 solution. Inset illustrates the principle of the VSL method where the sample is pumped with a stripe-shaped beam and ASE is extracted from the film edge. b) Fluorescence, ASE, and laser emission spectra of the host-guest complexed hydrogel film. c) Lasing efficiency of the hydrogel laser in the absence and presence of CB7. Inset illustrates the experimental conditions where the sample is immersed in an aqueous solution and pumped from below. d) Laser emission wavelength tuning is achieved by moving the pump spot along the thickness gradient on the sample.

measurement was carried out by keeping the pump spot the same throughout both series to exclude any variation based on the resonator parameters. The results revealed characteristic laser threshold behavior  $\approx 0.3 \mu\text{J}$  pump energy (fluence of  $74 \mu\text{J cm}^{-2}$  per pulse), with a slight decrease in threshold energy and a 30% increase in the slope efficiency in the presence of the host. As spot size and position remained the same, this can be linked again to the encapsulation of the RhBa molecules and the resulting higher radiative decay efficiency. Significantly better photostability combined with improved efficiency of the system induced by host-guest complexation provides interesting perspectives for hydrogel-based photonic devices as demands on the pump source are lowered and operational lifetime increases toward practical use. However, there is plenty of room left for optimization in material properties and device structures, such as laser resonators.

As an additional feature, the slanted resonator design allowed wavelength tuning based on the hydrogel layer thickness change. The thickness affects the effective refractive index  $n_{\text{eff}}$  of the waveguide and therefore the emission wavelength (Equation 1). Wavelength tuning from 624 nm to 642 nm is shown in Figure 4d by scanning the pump beam on the sample. Consequently, one of the key features of dye lasers can be readily achieved in the hydrogel gain material that combines the desired properties of the

solid and liquid environments. This brings the advantages of liquid and solid-state dye lasers together, such as heat dissipation, safety, material processability and integrability.

### 3. Conclusion

We have shown that the supramolecular host-guest complex between a fluorescent dye RhBa and a macrocyclic host CB7 leads to enhanced fluorescence in swollen PNIPAm-based hydrogel. Dye aggregates are separated into highly radiative monomeric species by CB7 encapsulation, causing a 5-fold increase in fluorescence emission intensity and the quantum yield growth from 17% to 51%. The supramolecular complexation further stabilizes the dye molecules by hindering the interactions that cause photodegradation, leading to substantially better photostability and providing prospects toward practical operation lifetimes. Furthermore, the covalent linking of the dye to the polymer network inhibits leaching and allows stable light emission while immersed in liquids. Based on the studied hydrogel, we fabricated a thin film DFB laser with wavelength tunability. Laser operation in underwater conditions was observed with a 30% increase in slope efficiency upon host addition. Furthermore, tunable emission from

624 nm to 642 nm demonstrates the potential of organic hydrogel lasers.

In the laser fabrication process, a combination of photo- and soft lithography techniques with photoinitiated free radical polymerization were used. These relatively fast and cost-effective fabrication processes, when combined with affordable hydrogels and dyes, allow scalability and rapid production of devices, with the added option for disposability. Furthermore, the malleability and mechanical flexibility of hydrogels make them easy to be integrated into field-ready systems such as chip laboratories. The responsive swelling offers additional possibilities for sample analysis as it allows the device framework to be enclosed within a solid network with analyte solution passing through simultaneously. Changes in material properties induced by swelling could be transformed and extracted as different signals, for example, laser emission demonstrated in current work. On the other hand, swelling could be used to control the laser emission via a specific stimulus, for example, temperature, light, pH, analytes, or electric/magnetic field. This opens possibilities to design responsive and controlled light sources for biocompatible optofluidic devices.

#### 4. Experimental Section

**Hydrogel Film Fabrication:** The hydrogel films were prepared via free-radical photopolymerization from a precursor solution inside a glass cell. First, precursor solution was prepared by dissolving *N*-isopropylacrylamide (86 mol-%), *N,N*-methylenebis(acrylamide) (8 mol-%), acrylic acid (5 mol-%), RhBa (0,5 mol-%) and 2,2-dimethoxy-2-phenylacetophenone (0,5 mol-%) in a 2:1 1,4-dioxane–water mixture with a total mass concentration of 500 mg mL<sup>-1</sup>. RhBa was synthesized in-house (see Supporting Information and Figure S7, Supporting Information) and other precursors were commercially available. CB7 was synthesized according to the literature.<sup>[59]</sup> To ensure thorough mixing, the solution was subsequently sonicated for 10 min at ambient temperature and purged with nitrogen for 10 min before use, to remove dissolved oxygen.

The polymerization cell was constructed from clean glass slides (sonication in acetone + IPA, 10 min each), cut to dimensions of approximately 2,6 cm × 2,6 cm. One substrate was treated with trimethoxy(silylpropyl) methacrylate (TMSPM) by soaking the substrate for 1 min in 1 vol-% of TMSPM in EtOH and subsequently rinsing with EtOH. The other substrate was treated with poly(vinyl alcohol) by spin coating (1 wt-% in water, 4000 rpm for 60 s, drying at 90 °C for 5 min) to ease the detachment of hydrogel film. Finally, the two glass slides were joined by adding UV-curable glue (UVS 91, Norland Products) mixed with 1 μm borosilicate glass spheres as spacers in the corners and gently pressing the top glass before curing with 365 nm LED (pE-4000, CoolLed). The resulting cell size was ≈2.6 cm × 1.5 cm.

The polymerization was carried out at ambient temperature by capillary filling of the cell and illuminating from the top with 365 nm LED at 1 mW cm<sup>-2</sup> intensity for 40 min under N<sub>2</sub>-flow. After polymerization, the cell was opened with a razor followed by rinsing the sample in water for 12 h to remove unreacted monomers. Finally, if required for characterization, samples were dried in a vacuum at 60 °C for 12 h.

**Hydrogel Laser Fabrication:** Master SRGs were inscribed on Disperse Red 1 glass (DR1g) film on a glass substrate, spin-coated from 6 wt-% dichloroethane solution at 3000 rpm for 45 s and subsequently dried in a vacuum at 40 °C for 1 h. The DR1g film was exposed to interfering p-polarized 488 nm laser beams (Genesis CX 488–2000 SLM, Coherent) in Lloyd's mirror configuration (5 min inscription at an intensity of 320 mW cm<sup>-2</sup>). The created master SRGs were then replicated on low-refractive index polymer MY133-V2000 (MyPolymers) by adding a drop of precursor on the master SRG and inserting a clean glass slide on top with 50 μm spacers (Scotch tape) and gently pressing on top. Subsequently,

MY133-V2000 film was cured with 365 nm LED at 20 mW cm<sup>-2</sup> for 10 min under N<sub>2</sub>-flow, after which the cell was carefully opened with a razor. Finally, MY133-V2000 SRG replicas were activated with oxygen plasma for 5 min (PDC-002, Harrick Plasma) and then treated with TMSPM. SRGs were characterized by atomic force microscope (Dimension Icon, Bruker)

A polydimethylsiloxane (PDMS) film with a thickness of 1 μm used as a spacer was created by spin coating diluted PDMS precursor (Sylgard, 10:1 base-curing agent in 20% *n*-hexane, 6000 rpm for 90 s) and cured for 10 min at 150 °C (Figure S8, Supporting Information). Once cured, half of the film was removed by scraping with a razor to create a 1-μm step on a glass substrate.

The hydrogel laser was polymerized by adding a drop of precursor solution on the MY133-V2000 replica, which was immediately pressed against a glass substrate with a PDMS spacer such that one edge of the MY133-V2000 film was on PDMS and the other one on glass, creating a slanted cavity. The sample was polymerized with 365 nm LED at 20 mW cm<sup>-2</sup> for 5 min under N<sub>2</sub>-flow. After polymerization, the cell was carefully opened and the sample was transferred onto a clean glass slide with tweezers hydrogel side facing up.

**Host Addition:** The CB7 host molecules were added into the hydrogel via diffusion by swelling the hydrogel/laser samples in an aqueous CB7 solution. The solutions were prepared by dissolving CB7 in water and sonicated for 10 min to ensure proper mixing. The complexation kinetics depend on the concentration and amount of the CB7 solution and the swelling dynamics of the hydrogel. The optimal combination deduced from the titration series was 0.8 mL of 0.9 mM CB7 solution for an initial precursor volume of up to 6 μL (Figure S2, Supporting Information).

**Optical Characterization:** The optical properties of solutions and hydrogel films were characterized via absorption (Cary 60 UV–vis, Agilent Technologies) and fluorescence (FLS1000, Edinburgh Instruments) spectroscopy. Hydrogels in a wet state were measured in a glass cell filled with an appropriate solution. QY of the hydrogel film was measured with a calibrated integrating sphere in combination with FLS1000 by confining a thin layer of liquid on top of the film and covering it with a glass slide (See Supporting Information for details). The excitation wavelength in fluorescence and QY measurements was 530 nm. The refractive index of the hydrogel was estimated with a refractometer (Abbebat 3200, Anton Paar).

Optical pumping of the hydrogel films and lasers was done with frequency tripled Nd:YAG laser (Quanta-Ray lab-130-10, Spectra-Physics, repetition rate of 10 Hz) operating an optical parametric oscillator (versaScan/MB, Spectra-Physics) that converted the output to 560 nm and 5 ns pulse. In gain measurements the sample was illuminated perpendicular to the surface with a stripe-shaped beam (fluence of 450 μJ cm<sup>-2</sup>) and emission was collected from the sample edge. Stripe dimensions were 100 μm × 3 mm (LBP2-H2-VIS2 beam profiler, Newport) and it was focused on the sample with increasing length by 100 μm steps. Photostability measurements were conducted with a fluence of 5.4 mJ cm<sup>-2</sup>. Lasing was studied on an inverted microscope (Zeiss) by setting the sample on a glass slide. The pump beam with a diameter of 360 μm and polarization parallel to grating lines was focused on the sample by a microscope objective from below and the emission signal was collected with the same objective and a beam splitter into a spectrometer (SR-303i-B/Newton CCD, Andor). All experiments were conducted in ambient conditions.

#### Supporting Information

Supporting Information is available from the Wiley Online Library or from the author.

#### Acknowledgements

The authors acknowledge the funding from the Academy of Finland through projects SUPREL (No. 311142 & 326416) and BioBase (No. 352900), Center of Excellence LIBER (No. 346107), and Flagship programme PREIN (No.320165). The authors are grateful to Tampere Microscopy Center for providing facilities for atomic force microscopy, Dr.

Suvi Lehtimäki for the help with AFM measurements, Dr. Nikita Durandin for the help with fluorescence measurements, and Dr. Tero-Petri Ruoko for helpful discussions.

## Conflict of Interest

The authors declare no conflict of interest.

## Data Availability Statement

The data that support the findings of this study are available from the corresponding author upon reasonable request.

## Keywords

fluorescence enhancement, fluorescent dyes, host–guest complexes, hydrogels, organic lasers, thin-film DFB lasers

Received: January 30, 2023

Revised: March 13, 2023

Published online: May 1, 2023

- [1] K. Kim, N. Selvapalam, Y. H. Ko, K. M. Park, D. Kim, J. Kim, *Chem. Soc. Rev.* **2007**, *36*, 267.
- [2] S. Y. Jon, N. Selvapalam, D. H. Oh, J.-K. Kang, S.-Y. Kim, Y. J. Jeon, J. W. Lee, K. Kim, *J. Am. Chem.* **2003**, *125*, 10186.
- [3] D. Wang, S. Wu, *Langmuir* **2016**, *32*, 632.
- [4] Y. Takashima, T. Sahara, T. Sekine, T. Kakuta, M. Nakahata, M. Otsubo, Y. Kobayashi, A. Harada, *Macromol Rapid Commun.* **2014**, *35*, 1646.
- [5] K. Iwaso, Y. Takashima, A. Harada, *Nat. Chem.* **2016**, *8*, 625.
- [6] R. Periasamy, *J. Carbohydr. Chem.* **2020**, *39*, 189.
- [7] A. S. Kuenstler, M. Lahikainen, H. Zhou, W. Xu, A. Priimagi, R. C. Hayward, *ACS Macro Lett.* **2020**, *9*, 1172.
- [8] K. Nobusawa, M. Akiyama, A. Ikeda, M. Natio, *J. Mater. Chem.* **2012**, *22*, 22610.
- [9] R. D. Mukhopadhyay, G. Das, A. Ajayaghosh, *Nat. Commun.* **2018**, *9*, 1987.
- [10] R. L. Halterman, J. L. Moore, W. T. Yip, *J. Fluoresc.* **2011**, *21*, 1467.
- [11] H. Sahoo, *RSC Adv.* **2012**, *2*, 7017.
- [12] D. Wu, A. C. Sedgwick, T. Gunnlaugsson, E. U. Akkaya, J. Yoon, T. D. James, *Chem. Soc. Rev.* **2017**, *46*, 7105.
- [13] A. J. C. Kuehne, M. C. Gather, *Chem. Rev.* **2016**, *116*, 12823.
- [14] O. Valdes-Aguilera, D. C. Neckers, *Acc. Chem. Res.* **1989**, *22*, 171.
- [15] M. Talhivini, T. D. Z. Atvars, *J. Photochem. Photobiol., A* **1998**, *114*, 65.
- [16] R. N. Dsouza, U. Pischel, W. M. Nau, *Chem Rev.* **2011**, *111*, 7941.
- [17] J. Mohanty, H. Pal, A. K. Ray, S. Kumar, W. M. Nau, *ChemPhysChem* **2007**, *8*, 54.
- [18] J. Mohanty, K. Jagtap, A. K. Ray, W. M. Nau, H. Pal, *ChemPhysChem* **2010**, *11*, 3333.
- [19] I. D. W. Samuel, G. A. Turnbull, *Chem. Rev.* **2007**, *107*, 1272.
- [20] S. Chénais, S. Forget, *Polym. Int.* **2011**, *61*, 390.
- [21] A. Rose, Z. Zhu, C. F. Madigan, T. M. Swager, V. Bulovic, *Nature* **2005**, *434*, 876.
- [22] F. J. Duarte, *Prog. Quantum Electron.* **2012**, *36*, 29.
- [23] R. Khurana, S. Agarwalla, G. Sridhar, N. Barooah, A. C. Bhasikuttan, J. Mohanty, *ChemPhysChem* **2018**, *19*, 2349.
- [24] H. Kogelnik, C. V. Shank, *Appl. Phys. Lett.* **1971**, *18*, 152.
- [25] A. Berdin, H. Rekola, O. Sakhno, M. Wegener, A. Priimagi, *Opt. Express* **2019**, *27*, 25634.
- [26] H. Coles, S. Morris, *Nat. Photon.* **2010**, *4*, 676.
- [27] H. Finkelmann, S. T. Kim, A. Muñoz, P. Palffy-Muhoray, B. Taheri, *Adv. Mater.* **2001**, *13*, 1069.
- [28] H. Lu, C. Wei, Q. Zhang, M. Xu, Y. Ding, G. Zhang, J. Zhu, K. Xie, X. Zhang, Z. Hu, L. Qiu, *Photon. Res.* **2019**, *7*, 137.
- [29] J. Mysliwiec, L. Sznitko, A. Sobolewska, S. Bartkiewicz, A. Miniewicz, *Appl. Phys. Lett.* **2010**, *96*, 141106.
- [30] L. M. Goldenberg, V. Lisinetskii, Y. Gritsai, J. Stumpe, S. Schrader, *Adv. Mater.* **2012**, *24*, 3339.
- [31] E. Yariv, S. Schultheiss, T. Saraidarov, R. Reisfeld, *Opt. Mater.* **2001**, *16*, 29.
- [32] X. Wang, X. Liu, X. Wang, *Sens. Actuators, B* **2014**, *204*, 611.
- [33] H. Mutian, W. Dong, W. Shuwang, M. Yanfei, A. Yousif, H. Ximin, *ACS Appl. Mater. Interfaces* **2021**, *13*, 12689.
- [34] A. Mourran, H. Zhang, R. Vinokur, M. Möller, *Adv. Mater.* **2017**, *29*, 1604825.
- [35] K. S. Soppimath, A. R. Kulkarni, T. M. Aminabhavi, *J. Controlled Release* **2001**, *75*, 331.
- [36] M. Mesch, C. Zhang, P. V. Braun, H. Giessen, *ACS Photonics* **2015**, *2*, 475.
- [37] X. Gong, Z. Qiao, Y. Liao, S. Zhu, L. Shi, M. Kim, Y.-C. Chen, *Adv. Mater.* **2022**, *34*, 2107809.
- [38] X. Gong, Z. Qiao, P. Guan, S. Feng, Z. Yuan, C. Huang, G.-E. Chang, Y.-C. Chen, *Adv. Photonics Res.* **2020**, *1*, 2000041.
- [39] T. Beck, M. Hauser, T. Grossmann, D. Floess, S. Schleede, J. Fischer, C. Vannahme, H. Kalt, *Proc. SPIE* **2010**, *7888*, 78880A.
- [40] C. Vannahme, S. Klinkhammer, U. Lemmer, T. Mappes, *Opt. Express* **2011**, *19*, 8179.
- [41] L. Yang, X. Fan, J. Zhang, J. Ju, *Polymers* **2020**, *12*, 389.
- [42] L. Tang, L. Wang, X. Yang, Y. Feng, Y. Li, W. Feng, *Prog. Mater. Sci.* **2021**, *115*, 100702.
- [43] N. Peppas, P. Bures, W. Leobandung, H. Ichikawa, *Eur. J. Pharm. Biopharm.* **2000**, *50*, 27.
- [44] Y. Wu, S. Joseph, N. R. Aluru, *J. Phys. Chem. B* **2009**, *113*, 3512.
- [45] M. Li, B. Bresson, F. Cousin, C. Fretigny, Y. Tran, *Langmuir* **2015**, *31*, 11516.
- [46] S. J. Lue, C.-H. Chen, C.-M. Shih, *J. Macromol. Sci., Part B: Phys.* **2011**, *50*, 563.
- [47] F. Biedermann, V. D. Uzunova, O. A. Schermann, W. M. Nau, *J. Am. Chem. Soc.* **2012**, *134*, 15318.
- [48] J. Mohanty, A. C. Bhasikuttan, W. M. Nau, H. Pal, *J. Phys. Chem. B* **2006**, *110*, 5132.
- [49] D. Setiawan, A. Kazaryan, M. A. Martoprawirob, M. Filatov, *Phys. Chem. Chem. Phys.* **2010**, *12*, 11238.
- [50] J. Mohanty, W. M. Nau, *Angew. Chem., Int. Ed.* **2005**, *44*, 3750.
- [51] W. M. Nau, J. Mohanty, *Intern. J. Photoenergy* **2005**, *7*, 133.
- [52] T. A. Martyn, J. L. Moore, R. L. Halterman, W. T. Yip, *J. Am. Chem. Soc.* **2007**, *129*, 10338.
- [53] E. M. Calzado, J. M. Villalvilla, P. G. Boj, J. A. Quintana, R. Gómez, J. L. Segura, M. A. D. García, *Appl. Opt.* **2007**, *46*, 3836.
- [54] L. M. Goldenberg, V. Lisinetskii, S. Schrader, *Adv. Opt. Mater.* **2013**, *1*, 527.
- [55] L. Rocha, V. Dumarcher, C. Denis, P. Raimond, C. Fiorini, J.-M. Nunzi, *J. Appl. Phys.* **2001**, *89*, 3067.
- [56] R. Kirby, R. G. Sabat, J.-M. Nunzi, O. Lebel, *J. Mater. Chem. C* **2014**, *2*, 841.
- [57] A. Natansohn, P. Rochon, *Chem. Rev.* **2002**, *102*, 4139.
- [58] L. Cerdán, *Opt. Lett.* **2017**, *42*, 5258.
- [59] C. Marquez, F. Huang, W. M. Nau, *IEEE Trans. Nanobiosci.* **2004**, *3*, 39.